

# LEAST-SQUARES SPECTRAL ELEMENT METHOD WITH IMPLICIT TIME INTEGRATION FOR THE INVISCID BURGERS EQUATION

G. Oldenziel\*, M.I. Gerritsma†

\*Delft University of Technology, Faculty of Aerospace Engineering  
Kluyverweg 1, 2629 HS Delft, The Netherlands  
e-mail: [g.oldenziel@student.tudelft.nl](mailto:g.oldenziel@student.tudelft.nl)

†Delft University of Technology, Faculty of Aerospace Engineering,  
Kluyverweg 1, 2629 HS Delft, The Netherlands  
e-mail: [m.i.gerritsma@tudelft.nl](mailto:m.i.gerritsma@tudelft.nl)

**Key words:** Least-Squares Spectral Element Methods, hyperbolic equations, *hp*-convergence

**Abstract.** *This paper describes the use of the Least-Squares Spectral Element Method for non-linear hyperbolic equations. The one-dimensional inviscid Burgers equation is specifically subject of investigation. A second order backward difference method is used for time stepping. The behaviour of this formulation is examined by application to a testcase where a moving shock develops. For this testcase an *hp*-convergence study is performed.*

## 1 INTRODUCTION

The Least-Squares Spectral Element Method (LS-SEM) combines the robust features of the Least-Squares Finite Element Method<sup>1</sup> (LS-FEM), with the high accuracy of the Spectral/*hp* Element Method<sup>2</sup>. Proot and Gerritsma<sup>3, 4</sup> and Pontaza and Reddy<sup>5, 6</sup> were the first to investigate this method. Given well-posedness, LS-SEM will transform any system of partial differential equations to a symmetric positive definite system of algebraic equations. For time dependant problems recently a space-time formulation was applied to a number of testcases<sup>7, 8</sup>. In this work an implicit time integration scheme is chosen. This is less intensive computationally compared to a space-time formulation but also less accurate.

Problems where shocks develop pose severe stability requirements on the approximation method and therefore often unphysical damping is used. This is not the case for LS-SEM. When a discontinuity is formed Gibbs-like oscillations do emerge but they don't tend to pollute the whole domain. They will stay in the vicinity of the discontinuity. If high accuracy around the shock is required it is possible to reconstruct the solution accurately<sup>8, 9</sup>.

The outline of this paper is as follows. In section 2 the LS-SEM formulation with its constituting parts, the Least-Squares minimisation method and the Spectral/*hp* element

method will be discussed. Then in section 3 the Burgers equation will be subjected to LS-SEM with implicit time stepping after the equation is linearised. Finally, results on a test case will be shown, where a moving shock develops. Conclusions will be drawn in Section 4.

## 2 LEAST-SQUARES SPECTRAL ELEMENT FORMULATION

### 2.1 Least-Squares Formulation

Consider following linear boundary value problem

$$\mathcal{L}\mathbf{u} = \mathbf{f} \quad \text{in } \Omega, \tag{1}$$

$$\mathcal{R}\mathbf{u} = \mathbf{g} \quad \text{on } \Gamma. \tag{2}$$

Here  $\mathcal{L}$  is a linear first order differential operator and  $\mathcal{R}$  is a linear algebraic boundary operator. In this work the residual of the boundary conditions is minimised along with the residual of the differential equation, thus enforcing the boundary conditions weakly. It will be assumed that the operator  $(\mathcal{L}, \mathcal{R})$  is a continuous mapping from the underlying function space  $X$  onto the space  $Y(\Omega) \times Y(\Gamma)$ . The least-squares formulation now seeks to minimize the residuals of (1) and (2) by finding a  $\mathbf{u}$  that minimizes the following functional:

$$\mathcal{J}(\mathbf{u}) = \frac{1}{2} (\|\mathcal{L}\mathbf{u} - \mathbf{f}\|_{Y(\Omega)}^2 + \|\mathcal{R}\mathbf{u} - \mathbf{g}\|_{Y(\Gamma)}^2). \tag{3}$$

So a  $\mathbf{u}$  must be found for which it holds that:

$$\lim_{\epsilon \rightarrow 0} \frac{d}{d\epsilon} \mathcal{J}(\mathbf{u} + \epsilon\mathbf{v}) = 0. \tag{4}$$

With  $\mathbf{v}$  a sufficiently smooth test function. We obtain:

$$(\mathcal{L}\mathbf{u}, \mathcal{L}\mathbf{v})_{Y(\Omega)} + (\mathcal{R}\mathbf{u}, \mathcal{R}\mathbf{v})_{Y(\Gamma)} = (\mathbf{f}, \mathcal{L}\mathbf{u})_{Y(\Omega)} + (\mathbf{g}, \mathcal{R}\mathbf{v})_{Y(\Gamma)}. \tag{5}$$

Or with  $\mathbf{f} = \mathbf{g} = 0$ :

$$(\mathcal{L}\mathbf{u}, \mathcal{L}\mathbf{v})_{Y(\Omega)} + (\mathcal{R}\mathbf{u}, \mathcal{R}\mathbf{v})_{Y(\Gamma)} = 0. \tag{6}$$

The minimisation will be done in the  $L^2$ -norm. It is not trivial that minimisation of the residual automatically leads to minimisation of the error. Generally for linear equations it is possible to show that the error will be minimised along with the residual but for non-linear equations this is hard to prove. In this work it will be assumed that minimisation of the residual does lead to minimisation of the error. Nevertheless proving this remains an issue of interest.

### 2.2 Spectral/ $hp$ elements

In order to discretise the variational problem the domain  $\Omega$  is divided into  $N_{el}$  elements. In each element the approximate solution  $u_e$  is expanded in continuous basis functions  $\phi_i$

$$u_e^P(\xi) = \sum_{i=0}^P \hat{u}_i \phi_i(\xi), \tag{7}$$

with  $\xi$  the coordinate of the standard domain to which every element is mapped,  $\xi \in [-1, 1]$ ,  $P$  the polynomial degree and  $\hat{u}_i$  the coefficients of the basis functions in the approximate solution. For the basis functions a nodal expansion through the Gauss-Lobatto-Legendre (GLL) collocation points is used<sup>2</sup>

$$\phi_i(\xi) = \begin{cases} \frac{1-\xi}{2}, & i = 0, \\ \left(\frac{1-\xi}{2}\right)\left(\frac{1+\xi}{2}\right)P_{i-1}^{1,1}(\xi), & 0 < i < P, \\ \frac{1+\xi}{2} & i = P. \end{cases} \quad (8)$$

where  $P_{i-1}^{1,1}(\xi)$  is the Jacobi polynomial  $P_{i-1}^{\alpha,\beta}(\xi)$  with  $\alpha = \beta = 1$ . Here the GLL-points  $\xi_i$  are the roots of the first derivative of the Legendre polynomial of degree  $P$  complemented by the boundary nodes of the standard domain. To evaluate the integrals in (6) Gauss-Lobatto quadrature is used

$$\int_{-1}^1 f(\xi)d\xi \approx \sum_{i=0}^Q w_i f(\xi_i), \quad (9)$$

with  $\xi_i$  the  $Q + 1$  GLL-roots and  $w_i$  the GLL-weights

$$w_i = \int_{-1}^1 h_i(\xi)d\xi, \quad (10)$$

with  $h_i$  the Lagrange interpolant through the GLL-points. It was shown that for equations where discontinuous solutions can occur the use of a larger number of integration points  $Q$  than the polynomial order  $P$  improves convergence<sup>10</sup>. Therefore in this work  $Q = \frac{3}{2}(P+1)$  is used.

### 3 BURGERS EQUATION

The inviscid Burgers equation with boundary and initial condition is given by

$$\frac{\partial u}{\partial t} + \frac{\partial u^2}{\partial x} = 0 \quad \text{in } [0, L] \times (0, T], \quad (11)$$

$$u(0, t) = 0 \quad \text{in } (0, T], \quad (12)$$

$$u(x, 0) = u_{in}(x) \text{ in } [0, L]. \quad (13)$$

In this section this equation will be linearised, the time derivative will be discretised and results of a testcase where the solution displays a moving shock will be discussed.

#### 3.1 Newton linearisation

First the non-linear term in (11) will be linearised. Let  $\delta u$  be the difference of two consecutive non-linear iteration steps

$$\delta u = u_{[k+1]} - u_{[k]} \quad (14)$$

where  $k$  denotes the iteration count. The nonlinear term in (11) can now be linearised by inserting (14) and neglecting terms of order  $\mathcal{O}((\delta u)^2)$

$$\begin{aligned}
 (u_{[k+1]})^2 &= (u_{[k]} + \delta u)^2 \\
 &= ((u_{[k]})^2 + 2u_{[k]}\delta u + (\delta u)^2) \\
 &\approx ((u_{[k]})^2 + 2u_{[k]}\delta u) \\
 &= ((u_{[k]})^2 + 2u_{[k]}(u_{[k+1]} - u_{[k]})) \\
 &= 2u_{[k]}u_{[k+1]} - (u_{[k]})^2.
 \end{aligned} \tag{15}$$

Inserting this in (11) yields the expression

$$\frac{\partial u}{\partial t} + 2u_{[k]}\frac{\partial u_{[k+1]}}{\partial x} + 2u_{[k+1]}\frac{\partial u_{[k]}}{\partial x} - 2u_{[k]}\frac{\partial u_{[k]}}{\partial x} = 0, \tag{16}$$

which is the Newton linearisation of the Burgers equation (11). The terms with subscript  $[k]$  will be iterated until convergence is reached at every timestep.

### 3.2 Implicit timestepping

Next the time derivative will be discretised using a second order backward difference scheme

$$\frac{\partial u}{\partial t} = \frac{3u^{n+1} - 4u^n + u^{n-1}}{2\Delta t} + \mathcal{O}(\Delta t^2), \tag{17}$$

where the superscript now denotes the different time-levels. This yields

$$\frac{3}{2}u_{[k+1]}^{n+1} - 2u^n + \frac{1}{2}u^{n-1} + \Delta t \left( 2u_{[k]}^{n+1}\frac{\partial u_{[k+1]}^{n+1}}{\partial x} + 2u_{[k+1]}^{n+1}\frac{\partial u_{[k]}^{n+1}}{\partial x} - 2u_{[k]}^{n+1}\frac{\partial u_{[k]}^{n+1}}{\partial x} \right) = 0. \tag{18}$$

With for the first iteration  $u_{[0]}^{n+1} = u^n$ . For the first timestep a first order backward difference scheme is used. The Least-Squares formulation of section 2.1 will now be employed to minimise the residual of (18).

### 3.3 Results

For the testcase the initial condition is given by

$$u_{in}(x) = \begin{cases} \frac{1}{2} - \frac{1}{2}\cos(\pi x) & \text{for } 0 \leq x \leq 2, \\ 0 & \text{elsewhere} \end{cases} \tag{19}$$

and the domain by  $[0, 4] \times (0, 2]$ . In Figure 1 the initial and final conditions are shown. Every timestep the solution is obtained iteratively until convergence is reached

$$|\Delta R| \leq tol, \tag{20}$$

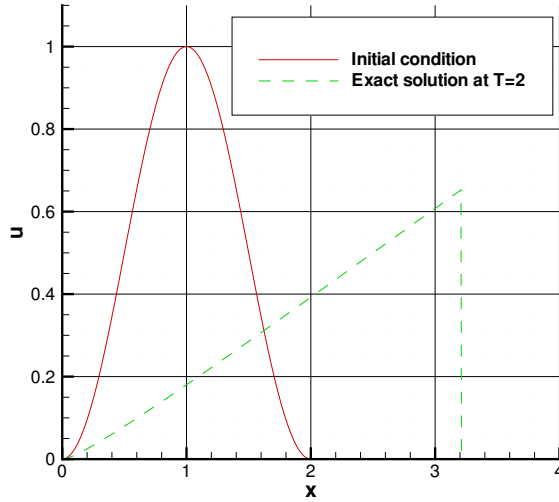


Figure 1: Initial condition and exact solution of the testcase.

with

$$\Delta R = \|R(u_{[k]})\|_{L^2} - \|R(u_{[k+1]})\|_{L^2}, \quad (21)$$

where  $tol = 1 \cdot 10^{-9}$  and

$$\|R(u)\|_{L^2} = \left( \int_0^4 (\mathcal{L}u - f)^2 dx \right)^{\frac{1}{2}}. \quad (22)$$

So  $\|R(u)\|_{L^2}$  is the  $L^2$ -norm of the residual. A simulation was performed with a timestep of  $\Delta t = 0.05$ . Figure 2 shows the LS-SEM solution with polynomial degree  $P = 7$  at the final timestep alongside the exact solution. It can be seen that the LS-SEM solution displays a smooth oscillation just left of the shock. The shock position is somewhat too far to the right initially and was observed to go to the left with increasing number of degrees of freedom.

For the same problem a  $hp$ -convergence study was performed, the results of which can be seen in Figures 3 and 4. Here  $R_{ave}$  is the sum of the residual at each timestep divided by the number of timesteps. Figure 4 shows initially a fast converging solution in the  $N_{el} = 8$  line of the  $L^2$ -error followed by a large increase in error. This behaviour was observed more often, especially for smaller values of  $\Delta t$ . In these cases initially the approximated shock position converges to a value close to the exact value from the left but suddenly the approximated shock position jumps to a location right of the exact value and the error starts converging. The jump to the right coincides with the increase in  $L^2$ -error. During the initial phase of this process the residual does not converge.

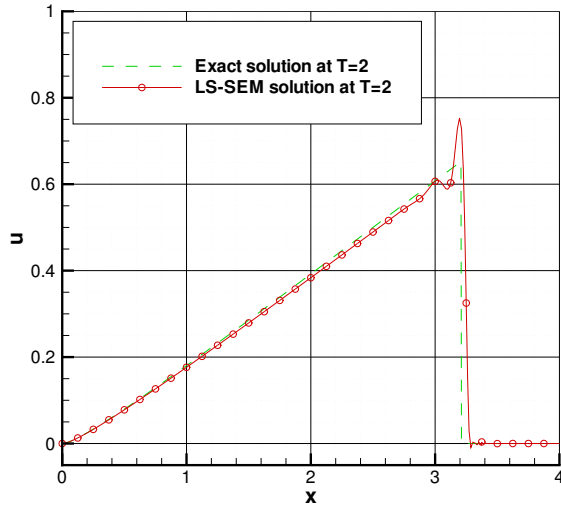


Figure 2: Exact and LS-SEM solution ( $N_{el} = 32, P = 7, Q = 12, \Delta t = 0.05$ ).

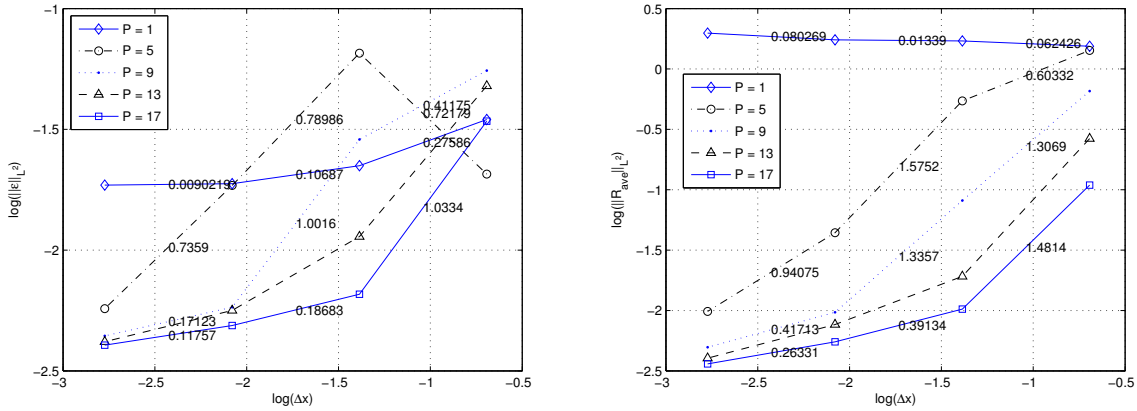


Figure 3:  $h$ -convergence of the error and averaged residual for  $\Delta t = 0.05$ . The numbers are the absolute values of the slope of the curves.

For all tested numbers of elements  $N_{el}$  from a certain point onwards the error decreases with increasing  $P$  as expected. In all figures at high numbers of degrees of freedom the lines seem to flatten out. The averaged residual displays a more smooth behaviour and also decreases with increasing  $P$ . A somewhat similar behaviour with increasing spatial resolution as with  $P$ -enrichment is shown by the error. In the behaviour of the residual an anomaly can be seen when refining  $\Delta x$ . For linear elements the residual seems to

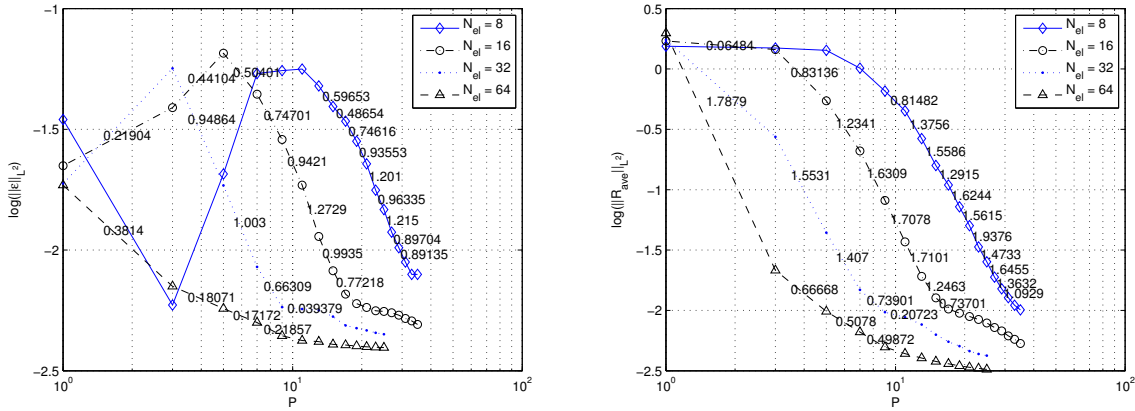


Figure 4:  $P$ -convergence of the error and averaged residual for  $\Delta t = 0.05$ . The numbers are the absolute values of the slope of the curves.

grow but decreasing the mesh size more was observed to lead to a decreasing residual. Whereas with smooth problems exponential convergence can be expected this is not the case here. For  $\Delta x$ -refinement as well as  $P$ -enrichment algebraic convergence occurs. In the clearly distinguishable convergent part of the lines the order of convergence of the residual is around 1.5 and that of the error is around 1.0. Convergence with polynomial enrichment is limited to algebraic convergence, because the underlying exact solution has limited regularity, thus preventing exponential convergence.

#### 4 CONCLUSIONS

The least-squares spectral element formulation with implicit time integration has been applied to the one dimensional inviscid Burgers equation. An initial condition has been used which gives rise to a solution where a moving shock develops. It has been observed that for every case convergence of the error and residual occurred. An interesting phenomenon in the process of convergence was observed. In the initial phase of  $P$ -enrichment on a mesh consisting of eight elements no convergence of the residual occurs and the error even diverges before the final trajectory towards convergence is reached. The LS-SEM approximation to the solution does show Gibbs-like oscillations but although no form of damping/stabilization/upwinding is required these oscillations never grow beyond the direct vicinity of the shock. Because of the very local nature of the large gradients in this problem an  $hp$ -adaptive algorithm is expected to reduce the amount of degrees of freedom in this problem considerably <sup>11</sup>.

**REFERENCES**

- [1] B.-N. Jiang. *The least square finite element method*, Springer, (2005).
- [2] G.E. Karniadakis and S. Sherwin. *Spectral/hp element methods for computational fluid dynamics*, Oxford Science Publications, second edition, (2005).
- [3] M.M.J. Proot and M.I. Gerritsma, A Least-Squares Spectral Element Formulation for the Stokes Problem, *J. Sci. Comp.*, **17**, 285–296, (2002).
- [4] M.M.J. Proot and M.I. Gerritsma, Least-Squares Spectral Elements Applied to the Stokes Problem, *J. Comp. Phys.*, **181**, 454–477, (2002).
- [5] J.P. Pontaza and J.N. Reddy. Spectral/hp least squares finite element formulation for the Navier-Stokes equation, *J. Comput. Phys.*, **190**, No. 2, 523–549, (2003).
- [6] J.P. Pontaza and J.N. Reddy. Spectral/hp Space-time coupled spectral/hp least-squares finite element formulation for the incompressible Navier-Stokes equation, *J. Comput. Phys.*, **197**, No. 2, 418–459, (2004).
- [7] B. De Maerschalck and M.I. Gerritsma. Space-Time Least-Squares Spectral Elements for Convection-Dominated Flows. *AIAA Journal*, **44**, No. 3, 558–565, (2006).
- [8] B. De Maerschalck and M.I. Gerritsma. The use of Chebyshev polynomials in the space-time least-squares spectral element method. *Num. Alg.*, **38**, 173–196, (2005).
- [9] D. Gottlieb and C.-W. Shu. On the Gibbs phenomenon and its resolution. *SIAM Rev.*, **38**, No. 4, 644–668, (1997).
- [10] B. De Maerschalck and M.I. Gerritsma. Higher-order Gauss-Lobatto integration for non-linear hyperbolic equations. *J. Sci. Comp.*, to appear, (2006).
- [11] A. Galvão, M.I. Gerritsma and B. De Maerschalck, hp-Adaptive Least Squares Spectral Element Method for Hyperbolic Partial Differential Equations, *J. Comp. and Appl. Math.*, to appear, (2006)